

Flow Control around Bluff Bodies by Attached Permeable Plates

G. M. Ozkan, H. Akilli

Abstract—The aim of present study is to control the unsteady flow structure downstream of a circular cylinder by use of attached permeable plates. Particle image velocimetry (PIV) technique and dye visualization experiments were performed in deep water and the flow characteristics were evaluated by means of time-averaged streamlines, Reynolds Shear Stress and Turbulent Kinetic Energy concentrations. The permeable plate was made of a chrome-nickel screen having a porosity value of $\beta=0.6$ and it was attached on the cylinder surface along its midspan. Five different angles were given to the plate ($\theta=0^\circ, 15^\circ, 30^\circ, 45^\circ, 60^\circ$) with respect to the centerline of the cylinder in order to examine its effect on the flow control. It was shown that the permeable plate is effective on elongating the vortex formation length and reducing the fluctuations in the wake region. Compared to the plain cylinder, the reductions in the values of maximum Reynolds shear stress and Turbulent Kinetic Energy were evaluated as 72.5% and 66%, respectively for the plate angles of $\theta=45^\circ$ and 60° which were also found to be suggested for applications concerning the vortex shedding and consequent Vortex-Induced Vibrations.

Keywords—Bluff body, flow control, permeable plate, PIV, VIV, vortex shedding.

I. INTRODUCTION

THE phenomenon of Vortex Induced Vibration (VIV) around bluff bodies is of practical interest of many fields in engineering since its output has several undesirable effects such as structural vibrations, increase in drag and lift forces on the body. If the frequency of VIV approaches to the natural frequency of bluff body, the case of resonance takes place and consequently sudden structural failures may occur. Although being an advantage for heat exchanger tubes, this is a serious problem in many engineering applications such as bridges, high-rise buildings, chimneys, turbine blades, cooling systems for nuclear power plants, power transmission lines etc. In recent years, investigations have been focused on applications in offshore engineering since oil risers (steel pipes) are being broken like a wire by large amplitude VIV's caused by the deep ocean currents. Ocean engineers are being busy with solving this problem because riser systems cost one-third of the entire offshore production unit. Beside this, pressure difference between the leading and trailing edges of the body increases, so the net drag force exerted on the body also increases which is also a disadvantage to be eliminated in the case of aerodynamics. Therefore, the effective control of VIVs is essential in engineering applications.

G. M. Ozkan and H. Akilli are with the Cukurova University, Faculty of Engineering & Architecture, Department of Mechanical Engineering, Adana, Turkey (phone: 90322-338-6084/2722, e-mail: gmozkan@cu.edu.tr, hakilli@cu.edu.tr).

Flow control can principally be achieved by controlling the separation of the boundary layer and various possible methods have been applied towards this aim, such as suction, blowing, surface roughness elements and splitter plate, etc. Therefore, many studies have been carried out in the past [1]-[12] to establish a method to control the vortex shedding which can be observed easily when fluid flows over a bluff body. A classification may be done by dividing the control methods into two categories, namely passive and active flow control. Passive control techniques modify a flow without external energy expenditure whereas active control ones apply some sorts of energy into the flow. As can be expected, passive control methods are cheaper and more applicable on the systems compared to other methods.

There are numerous investigations in the literature based on active and passive flow control. A good review by [13] presents control methods for flow over a bluff body such as a circular cylinder, a 2D bluff body with a blunt trailing edge, and a sphere. They introduced recent major achievements in bluff-body based flow controls such as 3D forcing, active feedback control, control based on local and global instability, and control with a synthetic jet. They also classified the controls as boundary-layer controls and direct-wake modifications and discuss important features associated with these controls.

One of the well-known methods for the passive control of the flow is to use a splitter plate placed downstream of the bluff body and some of the related scientific works utilizing a splitter plate were performed by [5]-[12]. The suppression of vortex shedding downstream of a cylinder was studied experimentally by [6]. In their work, the particle image velocimetry (PIV) technique was utilized for studying the flow characteristics of a circular cylinder placed in shallow water vertically. Vortex shedding due to the cylinder was controlled by the splitter plates with various lengths attached to the downstream base of the cylinder. It was determined by referring to the instantaneous and time-averaged flow data. The flow characteristics in the wake region of the cylinder were significantly influenced due to the length of the splitter plate. It was concluded that the flow characteristics substantially varied up to the splitter plate length to the cylinder diameter ratio of 1.0 and the longer splitter plates caused smaller changes in the wake region.

The study of [14] presents an example of flow control by using porous screens as shrouds around a cylinder in shallow water. They investigated the flow around a cylinder (inner cylinder) by a permeable outer cylinder having different porosities, β and diameter ratios, D/d . They stated that the

permeable outer cylinder suppresses the organized vortex street by reducing the velocity fluctuations in the near wake of the cylinder.

Aim of this study is to control the flow around a circular cylinder where the flow control will be done via a high-porosity ($\beta=0.6$) attached permeable plate (screen) along the span of the cylinder. The effect of plate angle θ , on flow control was studied where it can be defined as the angle between the plate and the centerline of the cylinder. This work will be an alternative passive control technique in suppressing or eliminating vortex induced vibrations in engineering applications.

II. EXPERIMENTAL METHOD

Experiments were performed in two sections; at the first part of the experiments dye visualization technique was used in order to have an idea about the flow structure downstream of the circular cylinder with permeable splitter plate. Throughout the second part, particle image velocimetry (PIV) technique was used to determine both instantaneous and the time-averaged velocity vector fields. Firstly the flow structure of a vertical cylinder with a diameter of $D=50\text{mm}$ was evaluated in order to see the effect of permeable splitter plate (screen) on the control vortex shedding behavior in deep water flow. Both dye visualization and PIV experiments were carried out in a recirculating open water channel having dimensions of $8000\text{ mm} \times 1000\text{ mm} \times 750\text{ mm}$ located at Fluid Mechanics Laboratory of Mechanical Engineering Department of Cukurova University.

Fig. 1 shows the schematic representation of the dimensions of cylinder diameter (D), plate angle with respect to centerline of the cylinder (θ), mesh size (a) and mesh diameter (t) and a formulation for the definition of porosity (i.e. the ratio of the gap area on the body to whole body surface area), β . The chrome-nickel screen, called as permeable plate in this study was attached on the cylinder surface having a porosity value of $\beta=0.6$ and a plate length to cylinder diameter ratio as $L/D=1.0$. The main parameter of this study is the plate angle and experiments were conducted for five different plate angles ($\theta=0^\circ, 15^\circ, 30^\circ, 45^\circ, 60^\circ$) in order to control the unsteady vortices downstream of the cylinder. Height of the water and free stream velocity was kept constant as $h_w=600\text{mm}$ and $U=95.2\text{mm/s}$ (corresponding to a Reynolds number of $Re=5000$), respectively.

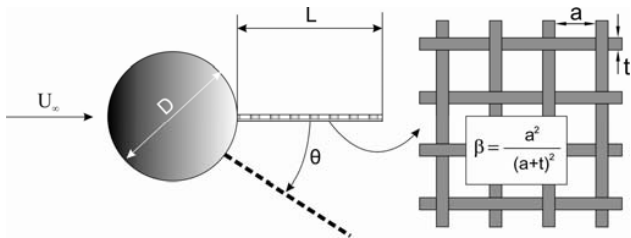


Fig. 1 Schematic presentation of the control technique and definition of porosity, β of permeable plate

Fig. 2 shows the plan view of PIV measurement system.

Streamline topology, instantaneous and mean velocity vector fields have been acquired by post-processing as well as Reynolds stress correlations. The ratio between the cylinder diameter and the width of the test section which is the geometric blockage of the cylinder was 5%. The flow of the water inside the channel was achieved using a pump driven by an electric motor having a variable speed controller. The experimental data was acquired and processed using Dantec Dynamics PIV system and Dynamic Studio Software installed on a computer.

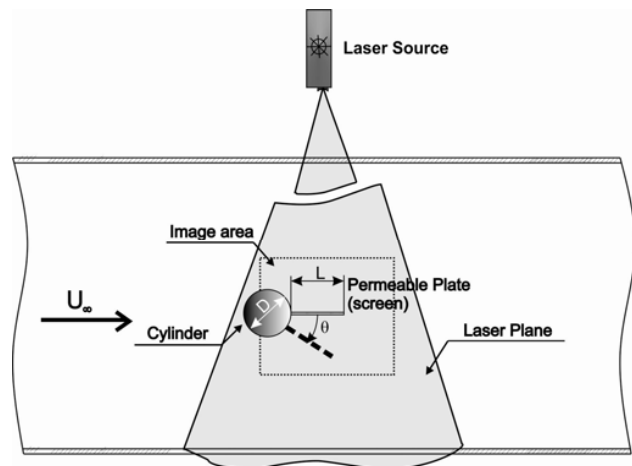


Fig. 2 Plan view of the measurement system

The measurement field was illuminated by a thin and intense laser light sheet by using a pair of double-pulsed Nd:YAG laser units each having a maximum energy output of 120mJ at 532nm wavelength. The laser sheet was oriented parallel to the bottom surface of the water channel and the experiments were carried out at the midplane of the water height. The image capturing was performed by an 8 bit cross-correlation charge-coupled device (CCD) camera having a resolution of $1600\text{ pixels} \times 1200\text{ pixels}$, equipped with a Nikon AF Micro 60 f/2.8 D lenses. In the image processing, 32×32 rectangular interrogation areas were used and an overlap of 50% was employed. The total 7326 (99×74) velocity vectors were obtained for an instantaneous velocity field at a rate of 15 frames/s . The overall view field was $219\text{ mm} \times 164\text{ mm}$ in physical size. The time interval between pulses was 1.75ms and the thickness of the laser sheet illuminating the measuring plane was nearly 2mm throughout the experiments. The values of time interval and the laser sheet thickness were selected to achieve the maximum amount of particles in the interrogation window. The uncertainty in velocity relative to depth-averaged velocity is about 2% in the present experiments. The water was seeded with $10\mu\text{m}$ diameter hollow glass sphere particles having a density of 1100kg/m^3 . In each experiment, 1000 instantaneous images were captured and recorded in order to have the time-averaged velocity vector field and other flow characteristics. Spurious velocity vectors were omitted using the local median-filter technique and replaced by using a bilinear least squares fit

technique between surrounding vectors.

III. RESULTS AND DISCUSSION

As mentioned before, dye visualization experiments were performed before quantitative PIV measurements in order to have some idea about the flow structure downstream of the cylinder. Fig. 3 presents the instantaneous dye visualization pictures for plain and permeable plate attached cylinders. Rolling up of the upper and lower shear layers and consequent vortex shedding is obviously seen for the plain cylinder. Attaching the permeable plate to the cylinder surface with a zero plate angle, $\theta=0^\circ$ results in a longer wake in which the starting point of vortex shedding occurs at farther regions of the wake compared to the plain cylinder. Further enlargement in the vortex shedding region was expected, however an interesting situation takes place for the case of $\theta=15^\circ$ where the vortex shedding now gets closer to the cylinder base compared to $\theta=0^\circ$. Increasing the plate angle to $\theta=30^\circ$ results in a larger wake width and longer vortex formation length. Vortices are rolled and shed at farther locations with respect to the previous cases, however the injection of fluid from the permeable plate to the wake region starts at the tip of the plate, which means further increase in the plate angle would result in greater amounts of momentum transfer from the lower shear layer through the meshes of the screen (permeable plate) as obvious for the cases of $\theta=45^\circ$ and 60° . The jet-like flow from the permeable plates effectively prevents the formation of a vortex on the lower shoulder of the cylinder, as well as rolling-up of the vortex formed on the upper shoulder of the cylinder. It can be concluded from these results that the cases of $\theta=45^\circ$ and 60° plate angles can be effective on suppression of the vortex shedding, however these qualitative results should be verified by the quantitative measurements which are presented on letter figures.

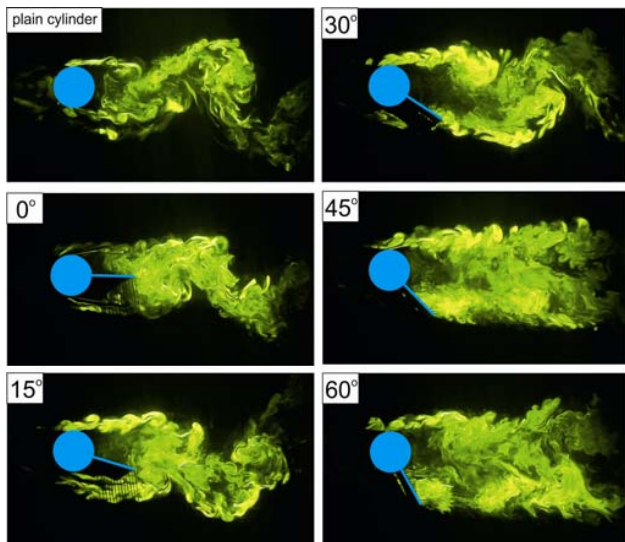


Fig. 3 Instantaneous dye visualization images for all cases

Fig. 4 presents the time- averaged streamline topologies, ψ ,

Reynolds shear stress, $\langle u'v' \rangle$ and Turbulent Kinetic Energy, TKE contours for all plate angles, as well as the plain cylinder case. The time- averaged streamlines for the plain cylinder are shown on the first row of the figure which defines two distinct foci, designated by F1 and F2 which are almost symmetrical with respect to the centerline of the cylinder. The saddle point, S is clearly observed approximately 1.3D away from the cylinder base. When the permeable plates attached on the cylinder span take place in order to control the unsteady flow structure, it is clearly seen from the results that streamline topologies are strongly affected by their presence, especially for $\theta \geq 30^\circ$ conditions. The cases of $\theta=0^\circ$ and 15° show a similar flow structure as the plain cylinder, i.e. the symmetrical flow structure is retained. However, the elongation in vortex formation region, which can be identified as the movement of saddle point in downstream direction, is changed compared to the plain cylinder. The saddle point is generated at 1.6D and 1.48 D away from the cylinder base for $\theta=0^\circ$ and 15° , respectively. After the plate angle of $\theta=30^\circ$, the flow structure dramatically changes; the foci F1 and F2 now take an asymmetrical shape due to the jet-like flows through the permeable plate in which an additional amount of momentum (on the plate side) is naturally injected into the wake region resulting in an elongation of the vortex formation region, namely the saddle points are generated at 1.84D, 2.12D and 2.24D away from the cylinder base for $\theta=30^\circ$, 45° and 60° , respectively. It can be concluded that these cases are effective on elongation in the vortex formation length which is an indication of suppression of vortex shedding.

One of the aims of flow control around bluff bodies is to reduce the fluctuations in the wake region of the body. Within this context, turbulence statistics such as Reynolds Shear stress and turbulent kinetic energy (TKE) were evaluated and compared to the plain cylinder. Second column of Fig. 4 shows the corresponding Reynolds Shear Stress correlations which have been made dimensionless by dividing them with the square of the depth- averaged free stream velocity U^2 , for better comparisons. On the figure, solid and dashed lines represent the positive and negative concentrations, respectively where the minimum and incremental values were taken as ± 0.1 and 0.001, respectively for all cases. The case for plain cylinder depicts that small- scale concentrations exist just behind the back stagnation point of the cylinder due to the small magnitude oscillations in that region. The amount of negative and positive concentrations gradually increases in downstream direction and reach to the peak values of -0.114 and 0.119, respectively. When the permeable plate attached to the cylinder surface takes place in order to control the flow structure, it is obviously seen from Fig. 4 that no significant change can be seen on the flow structure for the plate angles of $\theta=0^\circ$ and 15° except that slight asymmetry is observed due to the plate angle. Further increase in the angle to $\theta=30^\circ$ results in a sudden change on both shape and magnitude of Reynolds Shear stress concentrations in which a slight reduction exists. Further increase of the plate angle, θ demonstrates a great reduction in the concentrations of Reynolds Shear Stress values.

The third column of Fig. 4 demonstrates the spatial distribution of Turbulent Kinetic Energy, TKE where the minimum and incremental values were taken as 0.02 for all cases. Here the concentration of TKE slightly decreases by usage of the permeable plate except that small increase in the maximum value of TKE is valid for the case of $\theta=15^\circ$. For $\theta \geq 30^\circ$, the contours of TKE diminishes in downstream direction which can be an indication of the control of unsteady flow structure and consequent vortex induced vibrations, as well as elimination of the Karman Vortex Street which are all in conformity with the dye visualization experiments depicted by Fig. 3.

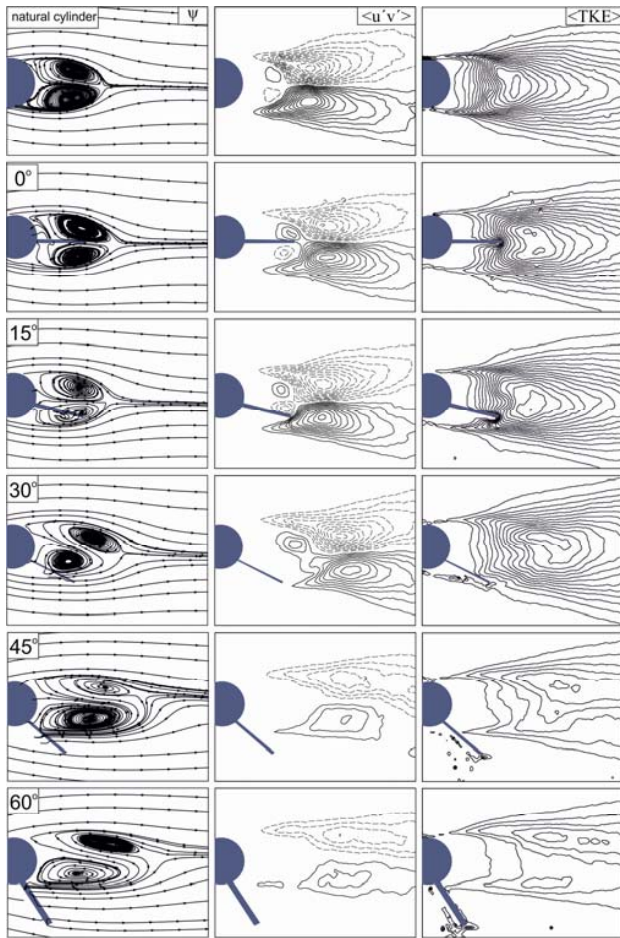


Fig. 4 Time- averaged streamline topologies ψ , Reynolds shear stress $\langle u'v' \rangle$, and Turbulent Kinetic Energy TKE, contours for all cases

In accordance with the concentrations, the maximum values of Reynolds Shear Stress and Turbulent Kinetic Energy evaluated in the flow field are shown in Figs. 5 (a) and (b), respectively. The maximum values for Reynolds Shear Stress were obtained by calculating the arithmetic mean of the absolute values of positive and negative peaks. Fig. 5 shows that the maximum values slightly decreases by existence of the permeable plate even for $\theta=0^\circ$ and 15° . As can be seen from

Fig. 4 (a), the permeable plate significantly reduces the maximum value of Reynolds Shear Stress for $\theta \geq 45^\circ$ approaching a maximum reduction of 72.5% for $\theta=60^\circ$ compared to the plain cylinder case. Similarly, the maximum value of Turbulent Kinetic Energy dramatically reduces by increasing plate angle and takes a maximum reduction by 66% for $\theta=60^\circ$ case compared to the plain cylinder. These results are effective indicators of the control of unsteady flow structure and consequent VIV's on bluff bodies.

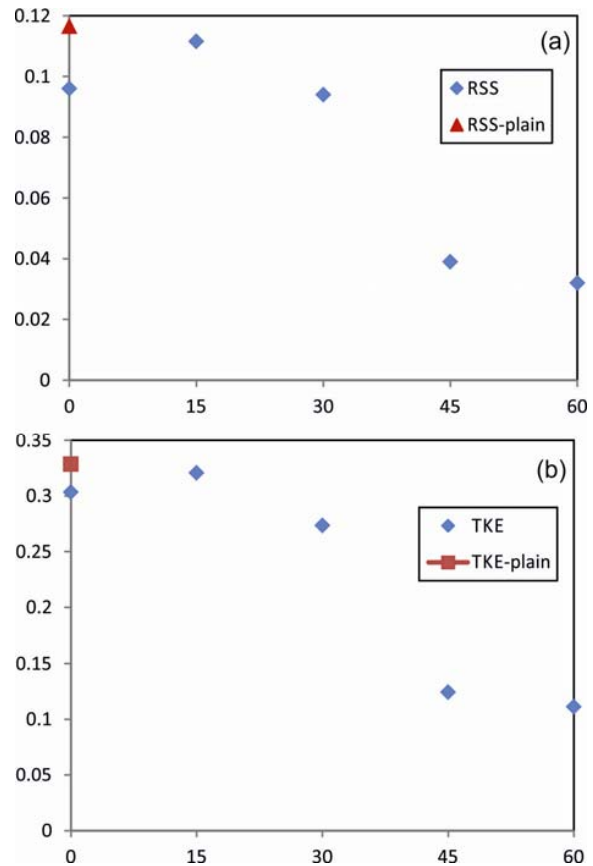


Fig. 5 Maximum values of Reynolds Shear Stress (a) and Turbulent Kinetic Energy (b) for all cases

IV. CONCLUSION

The flow structure downstream of a circular cylinder with attached permeable plates was investigated qualitatively and quantitatively using dye visualization and Particle Image Velocimetry techniques, respectively. The attached permeable plates constructed from screens having a porosity of $\beta=0.6$ were used with various plate angles θ , in order to control the unsteady vortical structure. The study showed that attachment of angled permeable plates (screens) was effective on suppression of vortex shedding and consequent Karman Vortex Street, as well as vibrations due to vortex shedding. Turbulence statistics and time- averaged streamlines evaluated from PIV measurements revealed that permeable plates with plate angles of $\theta=45^\circ$ and 60° significantly reduces the fluctuations in the wake region while elongating the vortex

formation length. This study might be an alternative method for passive control of vortex shedding around bluff bodies and elimination of Vortex Induced Vibrations.

REFERENCES

- [1] C. H. Kuo, L.C. Chiou, C. C. Chen, "Wake flow pattern modified by small control cylinders at low Reynolds number" in *Journal of Fluids and Structures*, vol. 23, pp. 938–956, 2007.
- [2] S. Mittal, A. Raghuvanshi, "Control of vortex shedding behind circular cylinder for flows at low Reynolds numbers" in *International Journal of Numerical Methods in Fluids*, vol. 35, pp. 421–447, 1999.
- [3] J.J. Wang, P.F. Zhang, S.F. Lu, K. Wu, "Drag reduction of a circular cylinder using an upstream rod" in *Flow, Turbulence and Combustion* vol. 76, pp. 83–101, 2006.
- [4] H. Baek, G.E. Karniadakis, "Suppressing vortex-induced vibrations via passive means" in *Journal of Fluids and Structures*, vol. 25, pp. 848–866, 2009.
- [5] B.G. Dehkordi, H.H. Jafari, "On the suppression of vortex shedding from circular cylinders using detached short splitter-plates" in *Journal of Fluid Eng-T ASME*, vol. 132, pp. 044501, 2010.
- [6] H. Akilli, C. Karakus, A. Akar, B. Sahin, N.F. Tumen, "Control of vortex shedding of circular cylinder in shallow water flow using an attached splitter plate" in *Journal of Fluid Engineering-T ASME*, vol. 130, pp. 041401, 2008.
- [7] H. Akilli, B. Sahin, N.F. Tumen, "Suppression of vortex shedding of circular cylinder in shallow water by a splitter plate" in *Flow Measurement Instrumentation*, vol. 16, pp. 211–219, 2005.
- [8] S. Turki, "Numerical simulation of passive control on vortex shedding behind square cylinder using splitter plate" in *Engineering Applications of Computational Fluid Mechanics*, vol. 2, pp. 514–524, 2008.
- [9] S.B. Yucel, O. Cetiner, M.F. Unal, "Interaction of circular cylinder wake with a short asymmetrically located downstream plate" in *Experiments in Fluids*, vol. 49, pp. 241–255, 2010.
- [10] K. Kwon, H. Choi, "Control of laminar vortex shedding behind a circular cylinder using splitter plates" in *Physics of Fluids*, vol. 8, pp. 479–486, 1996.
- [11] E. Rathakrishnan, "Effect of splitter-plate on bluff body drag" in *AIAA Journal*, vol. 37, pp. 1125–1126, 1999.
- [12] M.F. Unal, D. Rockwell, "On vortex formation from a cylinder Part 2: Control by splitter plate interference" in *Journal of Fluid Mechanics*, vol. 190, pp. 513–529, 1988.
- [13] H. Choi, W. Jeon, J. Kim, "Control of flow over a bluff body" in *Annual Review of Fluid Mechanics*, vol. 40, pp. 113–139, 2008.
- [14] G. M. Ozkan, V. Ouc, H. Akilli, B. Sahin, "Flow around a cylinder by a permeable outer cylinder in shallow water" in *Experiments in Fluids*, vol. 53, pp. 1751–1793, 2012.